Journal of Electroanalytical Chemistry 925 (2022) 116886

Contents lists available at ScienceDirect

Journal of Electroanalytical Chemistry

journal homepage: www.elsevier.com/locate/jelechem

Insight into the role of adsorbed formate in the oxidation of formic acid from pH-dependent experiments with Pt single-crystal electrodes

Mateusz J. Salamon [a], Valentín Briega-Martos [b,1], Angel Cuesta [a,c,*], Enrique Herrero [b,*]

[a] Department of Chemistry, School of Natural and Computing Sciences, University of Aberdeen, AB24 3UE Aberdeen, Scotland, UK
[b] Instituto de Electroquímica, Universidad de Alicante, E-03080 Alicante, Spain
[c] Centre for Energy Transition, University of Aberdeen, AB24 3FX Aberdeen, Scotland, UK

ARTICLE INFO

ABSTRACT

The concentration dependence of the activity for the oxidation of formic acid at pH 1.2, 2.4, and 3.9 has been studied on Pt(111), Pt(100), and stepped Pt[*n*(111) × (110)] electrodes. The results clearly demonstrate that, in this pH range, formate, and not formic acid, is the active species. To analyse the data, a kinetic model in which adsorbed monodentate formate is the active intermediate has been proposed. On Pt(111), a steady increase in the reaction rate with increasing pH and a reaction order of 1 for the bulk formate concentration was obtained, in agreement with the proposed model. On the other hand, the competition between adsorbed hydrogen and formate for the adsorption sites on Pt(100) cancels both the concentration and the pH dependence of the reaction rate. On this electrode, the potential dependence of the reaction rate for the dehydrogenation of formic acid to CO_{ad} was also studied and found to go through a maximum both at pH 1.2 and at pH 3.9, although the rate of dehydrogenation is slower and the maximum is broader at pH 3.9. The slower rate at the higher pH is consistent with the well-known fact that dehydrogenation of HCOOH is an acid-catalysed reaction. On Pt[*n*(111) × (110)] electrodes the behaviour observed is similar to that of Pt(111), with a reaction order of 1 for formate. The only significant difference with respect to the Pt(111) surface is the formation of CO_{ad} due to the presence of (110) steps.

1. Introduction

The oxidation of formic acid on Pt is undoubtedly a traditional topic in electrocatalysis. An obvious reason is the possibility of using formic acid as a liquid fuel in fuel cells. It is also an excellent example of how an apparently straightforward reaction (only two electrons and two protons need to be transferred and no new bond needs to be formed for its complete oxidation to CO_2) can proceed through a complex mechanism involving two parallel pathways [1]. Formic acid oxidation is also probably the best-known example of a non-linear electrochemical oscillator (actually, the oscillating behaviour of this reaction was known 23 years [2] before the discovery of the Belousov–Zhabotinsky reaction, the archetype non-linear chemical oscillator).

It is out of the question that the catalytic poison formed in the so-called indirect path of the reaction is adsorbed CO (CO_{ad}) and solid experimental evidence has cemented the consensus that monodentate adsorbed formate is the last intermediate in the direct path (see [3,4] and references therein). The more stable bidentate form of adsorbed formate is nonetheless not just a blocking species and therefore a dead end [5], as it can still affect the reactivity by being in equilibrium with the reactive intermediate and/or can contribute to stabilizing the reactive intermediate in its neighbourhood [4].

Actually, monodentate adsorbed formate has been shown to be the last intermediate common to both the direct and indirect pathways [6–8], *i.e.*, the crossroads where the reaction can choose which path to follow. Because formate, rather than formic acid, is the actual reactant [9–11], whatever the pathway, it is to be expected that both pathways will be affected by the pH of the electrolyte. In the case of the indirect pathway, a more substantial pH effect might be expected, because the dehydration of formic acid to gaseous carbon monoxide is a classic example of an acid-catalysed reaction. When the final product of the dehydration of formic acid is adsorbed CO (CO_{ad}, as opposed to gaseous CO produced by, *e.g.*, reacting HCOOH with concentrated sulphuric acid), we have shown [6–8,12] that the reaction involves an oxidation step ($HCOOH \rightleftharpoons HCOO_{ad} + H^+ + e^-$) followed

* Corresponding authors.
E-mail addresses: angel.cuestaciscar@abdn.ac.uk (A. Cuesta), herrero@ua.es (E. Herrero).
[1] Present address: Forschungszentrum Jülich GmbH, Helmholtz Institute Erlangen-Nürnberg for Renewable Energy (IEK-11), Cauerstr. 1, 91058 Erlangen, Germany.

https://doi.org/10.1016/j.jelechem.2022.116886
Received 9 September 2022; Received in revised form 5 October 2022; Accepted 6 October 2022
Available online 10 October 2022

by a reduction one ($HCOO_{ad} + H^+ + e^- \rightleftharpoons CO_{ad} + H_2O$), a very simple, *avant la lettre*, example of so-called catalysis by electrons [13–15], in this case, aided by catalysis by protons.

Building up on our recent work [8], we report here a detailed study of the effect of pH on the concentration dependence of the kinetics of the direct and indirect pathways of formic acid oxidation on Pt(1 1 1) and Pt(1 0 0) single-crystal electrodes. Pt(1 1 1) and Pt(1 0 0) electrodes represent two limit behaviours for the formic acid oxidation reaction at pH 1, and the pH dependence of the reaction rates can help understand these differences. Having established the different effects of pH and concentration on the Pt(1 1 1) and Pt(1 0 0) electrodes, we analyse the effect of pH on the reaction rate on surfaces belonging to the [(*n*-1) (1 1 1)×(1 1 0)] series (Pt(n,n,n-2) Miller indexes), *i.e.*, surfaces composed of (1 1 1) terraces *n* rows wide separated by (1 1 0) steps, in order to better understand the behaviour of polycrystalline Pt surfaces.

2. Experimental.

Pt(1 1 1) and Pt(1 0 0) single-crystal electrodes were prepared from single crystal beads formed by melting a 99.99 % Pt wire according to the procedure described by Clavilier [16]. Before use, single crystal electrodes were flame annealed, cooled in an Ar/H_2 (3:1) atmosphere, and protected with an ultrapure water drop saturated with these gases. This preparation procedure assures the cleanliness of the surface and that the obtained experimental surfaces correspond to the nominal topographies [17]. A two-compartment cell equipped with a Pt counter electrode and a reversible hydrogen electrode (RHE) as reference was used for pH 1 solutions and a Ag/AgCl for the rest of the solutions. In all cases, the electrode potential is quoted vs the RHE electrode unless otherwise indicated.

The solutions were prepared using 60 % $HClO_4$ (Merck, for analysis), HCOOH (Merck, for analysis), NaHCOO (Merck, Suprapur, 99.99 %) NaF (Merck, Suprapur, 99.99 %), H_2SO_4 (Merck, Suprapur), and ultrapure water (Elga PureLab Ultra, 18.2 MΩ cm). Solutions with pH 1.2 were prepared with 0.1 M $HClO_4$, whereas buffered solutions at pH 2.4 and 3.9 were prepared using mixtures of $HClO_4$ and NaF with a total concentration of 0.1 M. In these cases, the effect of formic acid/-formate concentration in its oxidation reaction was studied by adding mixtures of HCOOH/NaHCOO with the same pH to avoid altering the pH. Neither perchlorate nor fluoride adsorbs specifically on platinum electrodes and therefore they are not expected to interfere with the oxidation of formic acid [18].

Electrochemical measurements were carried out by using a signal generator (EG&G PARC) and an eDAQ EA161 potentiostat with an Edaq e-corder ED401 recording system. Experiments in hydrodynamic conditions were performed with the hanging-meniscus rotating disk electrode (HMRDE) configuration using an EDI101 rotating electrode and a Radiometer CTV 101 for controlling the rotation rate (both from Radiometer Analytical). All experiments were carried out at room temperature.

3. Results and discussion

The activity for the Pt(1 1 1) surface for formic acid oxidation is the lowest among the three basal planes, with a negligible reaction rate of CO_{ad} formation, whereas the activity for both paths is maximum for the Pt(1 0 0) electrode [19,20]. These two surfaces also show different trends when increasing the total formic acid concentration [8]. On Pt (1 1 1), the current increases, and the onset potential shifts negatively with increasing concentration, as expected if the rate is controlled by the kinetics of the rate-determining step. On the contrary, on Pt(1 0 0) the current is essentially independent of formic acid concentration between 0.05 and 0.75 M, suggesting that the rate of the reaction is controlled by the availability of the reactant. At the peak current, all the available sites are occupied by the active intermediate (monodentate adsorbed formate), and only when a CO_2 molecule is released can a new reacting species occupy the site left behind.

Fig. 1 shows the evolution of the voltammetric profile of Pt(1 1 1) with increasing total formic acid concentration at pH 1.2, 2.4, and 3.9. At all three pHs, the current increases with increasing concentration. Hysteresis between the positive and negative scan direction is also negligible in all cases, implying that very little CO_{ad} is being formed on this surface in all cases. This is consistent with previous work using stepped surfaces containing (1 1 1) terraces, which showed that the formation of CO_{ad} on Pt(1 1 1) electrodes occurs nearly exclusively on defects [19,21]. Thus, currents measured for this electrode correspond exclusively to the so-called direct pathway.

As illustrated by the change in the current scales in Fig. 1, the oxidation current also increases with increasing pH, which is accompanied by a significant change in the shape of the voltammetric profile. At pH 1.2 and 0.1 M formic acid concentration, the current at room temperature reaches a plateau between 0.4 and 0.6 V. As the concentration increases, a peak at 0.4 V begins to emerge. In temperature-dependent studies [22], the apparent plateau evolves into two well-defined peaks at 0.4 and 0.6 V, indicating two coverage-dependent possible reaction environments for adsorbed formate as an effect of the surface charge density, which affects the binding mode of monodentate adsorbed formate. As the pH increases, the shape evolves to one in which the currents for the oxidation peak at lower potentials increase significantly, dominating the whole voltammetric profile. It should be noted that the current plateau between 0.4 and 0.6 V is only observed in a small range of pH around 1 and formic acid concentrations around 0.1 M. Otherwise, the signal at 0.4 V is the most

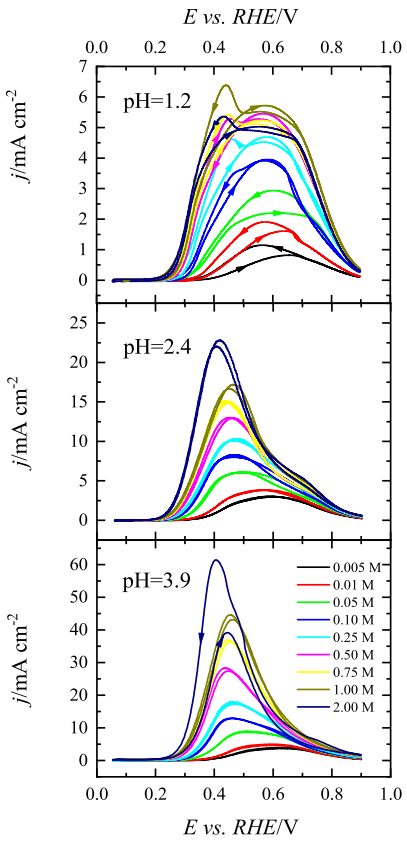

Fig. 1. Evolution of the voltammetric profile of the Pt(1 1 1) electrode in HMRDE configuration with increasing total formic acid concentration in $HClO_4$/NaF buffered solutions of pH 1.2 (top), 2.4 (middle), and 3.9 (bottom). Arrows indicate the scan direction when significant differences in the currents between positive and negative scan directions are observed. Scan rate: 50 mV s^{-1}, rotation rate: 1600 rpm.

prominent. At $E > 0.6$ V vs RHE, the current is essentially independent of the pH (Fig. S1).

This behaviour can be interpreted in light of the proposed oxidation mechanism for the formic acid oxidation reaction through the active intermediate. Thus, the following mechanism for the active reaction path can be proposed:

$$HCOOH \rightleftharpoons HCOO^- + H^+ \quad (1)$$

$$* + HCOO^- \rightleftharpoons HCOO_m + e^- \quad (2)$$

$$HCOO_m \rightarrow * + CO_2 + H^+ + e^- \quad rds \quad (3)$$

$$HCOO_m \rightleftharpoons HCOO_b \quad (4)$$

where $HCOO_b$ and $HCOO_m$ stand for bridge-bonded and monodentate adsorbed formate, respectively, and * represents an adsorption site on the surface for formate. Although the bonding of both formate adsorbed species is different, the area on the electrode surface blocked by them is the same, and thus, both configurations require the same number of sites to adsorb. In this mechanism, reaction (1) corresponds to the equilibrium between bulk formic acid and bulk formate, whereas reaction (2) is the first stage towards forming the bidentate formate layer. From here, the mechanism presents a bifurcation. Monodentate adsorbed formate either evolves to the stable bidentate form (reaction (4)) or yields CO_2 (reaction (3)) by breaking the C—H bond. Thus, the measured current will be:

$$i \propto k_3\theta_m(1 - \theta_b - \theta_m) \quad (5)$$

where k_3 is the potential-dependent rate constant of step (3). The value for θ_b will be determined by the rates of reaction (4), assuming that this step is in equilibrium:

$$k_4\theta_m = k_{-4}\theta_b \Rightarrow \theta_b = \frac{k_4}{k_{-4}}\theta_m \quad (6)$$

Assuming that $\theta_m \ll \theta_b$, the current is then:

$$i \propto k_3\theta_m(1 - \theta_b) = k_3\theta_m\left(1 - \frac{k_4}{k_{-4}}\theta_m\right) \quad (7)$$

The coverage of the monodentate form can be calculated from equilibrium (2), assuming that adsorption obeys the Langmuir isotherm (which will be true at sufficiently low coverage):

$$k_2(1 - \theta_m - \theta_b)c_{HCOO^-} = k_{-2}\theta_m \quad (8)$$

Assuming again that $\theta_m \ll \theta_b$, substituting the value of θ_b from equation (6) and solving for θ_m, transforms equation (7) into:

$$i \propto k_3 \frac{\frac{k_2}{k_{-2}}c_{HCOO^-}}{\left(1 + \frac{k_2}{k_{-2}}\frac{k_4}{k_{-4}}c_{HCOO^-}\right)^2} \quad (9)$$

In all these equations, the rate constants k_2, k_{-2}, and k_3 are potential dependent since electrons are transferred in these steps. Equation (9) predicts a complex dependence on the concentration of formate and a plot of log(i) vs log(c_{HCOO^-}) will, in principle, not be linear. However, under two limiting cases, linear plots can be obtained. At very low potentials, that is, close to the onset potential for the reaction, the formate coverage will be very low and $1 - \theta_b \approx 1$. Under these circumstances, it can be shown that $1 >> \frac{k_2}{k_{-2}}\frac{k_4}{k_{-4}}c_{HCOO^-}$ and equation (9) simplifies to:

$$i \propto k_3\frac{k_2}{k_{-2}}c_{HCOO^-} \quad (10)$$

which gives a reaction order for formate of 1. On the other hand, at high potential, where the reaction is highly inhibited because the formate coverage is close to 1 ($\theta_b \approx 1$) and therefore $1 << \frac{k_2}{k_{-2}}\frac{k_4}{k_{-4}}c_{HCOO^-}$, equation (9) transforms into:

$$i \propto k_3\frac{k_{-4}}{k_4} \quad (11)$$

In this case, the current will be independent of the formate concentration. In fact, as can be seen in Figs. 1, 4, and 5, at high potentials, the currents for the different concentrations almost overlap, in agreement with this model. Also, if θ_m in equation (6) is solved and substituted in equation (5) the model predicts that the currents will be proportional to.

$$i \propto k_3\frac{k_{-4}}{k_4}\theta_b(1 - \theta_b) \quad (12)$$

For the Pt(1 1 1) electrode and using the θ_b values obtained from fast scan measurements, a very good agreement has been found between the experimental and voltammetric currents calculated using equation (12) [23].

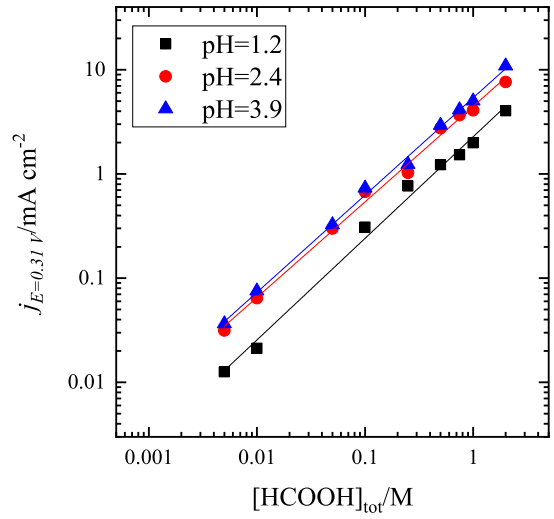

Fig. 2. Double logarithmic plot of the dependence of the formic acid/formate oxidation current at 0.31 V vs RHE on the total formic acid concentration on the Pt(1 1 1) electrode. Data correspond to experiments at pH 1 (black squares), 2.4 (red circles), and 3.9 (blue triangles).

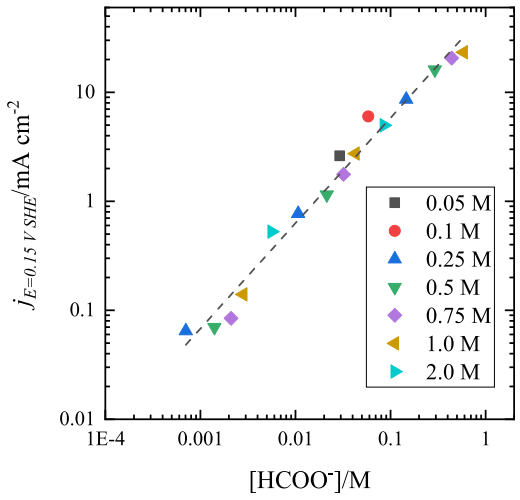

Fig. 3. Double logarithmic plot of the current density at 0.15 V vs SHE as a function of the free formate concentration in the solution on the Pt(1 1 1) electrode. Solutions pH with pH 1.2, 2.4, and 3.9 with a total formic acid concentration between 0.05 and 2 M were used. The different symbols refer to the total formic acid concentration.

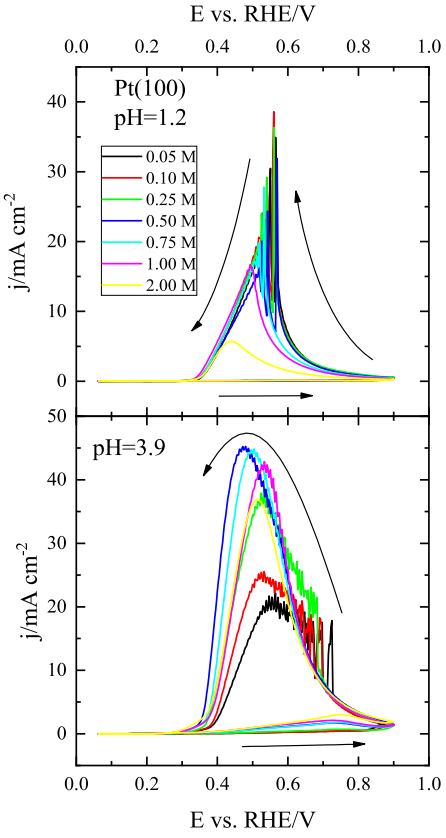

Fig. 4. Evolution of the voltammetric profile for the Pt(1 0 0) electrode in HMRDE configuration with the total formic acid concentration in pH 1.2 (top) and 3.9 (bottom) $HClO_4$/NaF buffered solutions. Arrows indicate the scan direction. Scan rate: 50 mV s^{-1}; rotation rate: 1600 rpm.

According to equation (10), a plot of the log(j) vs log([$HCOO^-$]) at constant E should be linear with a slope of 1 for potentials where $\theta_b \ll 1$, that is, close to the onset potential. Fig. 2 shows a double logarithmic plot of j vs $[HCOOH]_{tot}$ at 0.31 V in the positive scan direction vs RHE for the three pH values in Fig. 1. For this plot, currents have been corrected by the measured current at the same potential in the supporting electrolyte. At constant pH, $[HCOOH]_{tot}$ is proportional to [$HCOO^-$] and the slopes of j vs log$[HCOOH]_{tot}$ are between 0.91 and 0.97, which agrees with the proposed mechanism. A slope of 0.66 has been recently reported [8], but the fitting was restricted to higher concentrations, and currents were not corrected by the background. Had the currents been corrected and concentrations up to 0.5 M formic acid been included in the plot, a slope of 0.85 would have been obtained, in reasonable agreement with the present results. Special care has been taken in the present manuscript when recording the currents for high formic acid concentrations since they are prone to contamination from the commercial formic acid used to prepare the solutions.

This analysis can be extended to a wider set of data by plotting together the currents from solutions with different pH at constant potential vs SHE vs [$HCOO^-$] since formate is the active species. For that purpose, the concentration of formate in each specific solution with a given total formic acid/formate concentration and a given pH was calculated, and the logarithm of the current density at 0.15 V vs SHE was plotted against the logarithm of the calculated formate concentration. This potential value was selected because it is located in the rising part of the curve (see Figure S1), where the assumptions used to derive equation (10) are valid. As can be seen in Fig. 3, the double logarithm plot yields a straight line with a slope of 0.97 ± 0.04, which confirms the reaction order of 1 for formate, and corroborates the role of formate, rather than formic acid, as the active species in the reaction.

For the Pt(1 0 0) electrode, the pH behaviour is different from that observed with Pt(1 1 1), as shown in Fig. 4. In this case, the indirect path leading to CO_2 through the CO_{ad} catalytic poison is active. CO_{ad} formed in the most negative potential blocks the surface, leading to almost negligible oxidation currents in the positive scan direction. Once CO_{ad} is oxidized around 0.7 V, the electrode recovers its activity and positive currents that increase down to ca. 0.5 V are recorded in the negative scan direction. From this point, the current decreases due to the combined result of the less positive potential and the formation of CO_{ad}. Formic acid oxidation is well-known for displaying oscillatory behaviour when far from equilibrium [24,25]. These oscillations are clearly visible in Fig. 4 under the right conditions.

As reported recently [8], the current corresponding to the direct path of formic acid oxidation on Pt(1 0 0) at pH 1.2 is almost independent of the total formic acid concentration in the range between 1 M and 0.05 M. A decrease in the oxidation current is observed for $[HCOOH]_{tot} = 2$ M, which we attribute to impurities in the commercial formic acid used to prepare our solutions. Please note that Pt(1 0 0) is more prone to contamination than Pt(1 1 1). The same qualitative behaviour is observed at pH 3.9: negligible current in the positive scan direction due to the formation of CO_{ad} and significant but, in the range between 1 and 0.05 M, concentration-independent current in the negative scan direction. However, while a large increase in the current was observed with Pt(1 1 1) with increasing pH, with Pt(1 0 0) the pH-induced current increase is significantly smaller. Since voltammetric currents are affected by the CO_{ad} formation rate, which can also depend on the pH, this effect can mask the current increase through the active intermediate. Therefore, it is essential to determine reaction rates for both paths independently. Pulsed voltammetry was used for that purpose. In this technique, a short pulse to 0.85 V, in which CO_{ad} is oxidized, is superimposed to the staircase scan, and the current transient after the pulse is recorded. Extrapolation of the current to $t = 0$ provides the reaction rate for the active intermediate path, whereas the rate formation of CO_{ad} can be obtained from the current–time decay curve if an adequate model is applied [20].

The potential dependence of the extrapolated currents at $t = 0$ for pH 1.2 and 3.9 are shown in Fig. 5. As can be seen, currents show a very small concentration dependence in the range between 0.05 and 1 M for both pH values. Moreover, the maximum currents are nearly the same for both pHs. The only difference is that the oxidation peak for pH 3.9 is somehow broader because the decay at $E > 0.5$ V is less pronounced (Figure S2). On the other hand, CO_{ad} formation rates show important differences (Fig. 5). At pH 1.2, maximum rates are centered in a narrow region around the potential of zero total charge (pztc) of the electrode. On the other hand, at pH 3.9, the region where CO_{ad} is formed is wider, and the maximum rate is smaller than that measured for pH 1.2. This is not very surprising because the dehydration of formic acid to gaseous CO is known to be an acid-catalysed reaction [26]. However, outside the region around the pztc, rates for pH 3.9 are larger. These differences explain the observed voltammetric behaviour. The higher CO_{ad} formation rates around 0.4 V in pH 1.2 should lead to a more significant decrease of the voltammetric current negative of this potential and, therefore, lower voltammetric currents than at pH 3.9. However, similar values are obtained when the activity for the direct path for both electrodes is compared. The differences in the shape of the current curves have to be assigned to the effect of pH on the formate adsorption. As the pH increases, formate adsorption shifts to more negative potential values in the SHE scale (Fig. S3). Formate adsorption on Pt(1 0 0) competes strongly with hydrogen and thus the onset of the oxidation is marked by the point at which the replacement of hydrogen by formate takes place. For pH values lower than the pK_a of formic acid, both processes shift 59 mV to lower values per pH unit in the SHE scale. This fact implies that the electrode surface charge in the region where the oxidation takes place becomes more

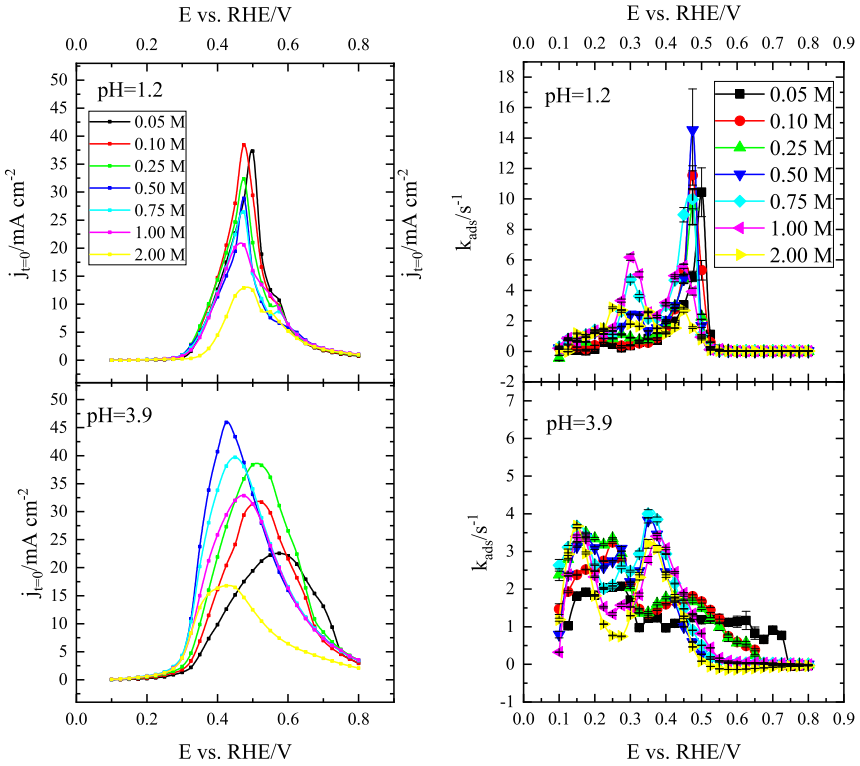

Fig. 5. Potential dependence of $j_{t=o}$ (left) and k_{ads} (right) for the oxidation of formic acid on the Pt(100) electrode as obtained from pulsed voltammetry experiments at pH 1.2 (top) and 3.9 (bottom).

negative with increasing pH, which must affect the adsorption and oxidation of formate. This effect can be observed in Fig. 5. At pH 1.2, the $j_{t=o}$ curves for the concentration range between 0.05 and 1 M almost overlap between 0.3 and 0.5 V, which is the part of the curve affected by the competition between the proton and formate for the adsorption. On the other hand, at pH 3.9, the onset potential shifts negatively with increasing concentration, because of the effect of negative surface charge on the adsorption of formate, which favours hydrogen adsorption in its competition with formate. Unfortunately, the interference of hydrogen adsorption on the oxidation process prevents determining the reaction order. However, this interference explains the very small dependence of the current on the formate concentration. When hydrogen is adsorbed, equation (12) should take into account the hydrogen coverage (θ_H), and the equation is transformed into:

$$i \propto k_3 \frac{k_{-4}}{k_4} \theta_b (1 - \theta_H - \theta_b) \tag{13}$$

At sufficiently negative potentials $1 - \theta_H - \theta_b \approx 1 - \theta_H$ and thus $i \propto \theta_b(1 - \theta_H)$. The current for the formic acid oxidation is then determined by the bidentate formate and hydrogen coverage. Those coverages are challenging to measure due to the overlapping oxidation process with large currents [8]. However, the adsorption of bidentate formate should be very similar to that of acetate. In the case of acetate, the increase in acetate concentration from 1 mM to 10 mM in 0.1 M $HClO_4$ results only in a small shift (ca. 10 mV) in the potential of the peak related to the replacement of hydrogen by adsorbed acetate [27,28]. This fact suggests that strong competition between formate and hydrogen for the adsorption sites should be expected, resulting in adsorption profiles that show little dependence on the concentration. Thus, in the region where hydrogen is co-adsorbed with formate, the $\theta_b(1 - \theta_H)$ term is nearly independent of the concentration of formate at a given potential, resulting in currents with a small dependence, if any, on the formate concentration.

For pH 3.9 some changes are observed. It should be taken into account that, in the RHE scale, the potential for hydrogen adsorption is pH-independent. On the other hand, formate adsorption is potential independent for pH < pK_a, whereas it should shift 59 mV in the RHE scale per pH unit when pH > pK_a [12] For pH 3.9, a pH value, which is slightly higher than the pK_a, the competition between hydrogen and formate is somehow weaker, especially for low formate concentrations and thus a displacement of the oxidation wave to lower potentials is observed when increasing the concentration.

Once the behaviour of the Pt(111) and Pt(100) has been analysed, stepped surfaces with (111) terraces will be examined next. It should be noted that the peak corresponding to the steps in the blank voltammogram appears at the same potential as that corresponding to the (110) sites on the polycrystalline samples, which are the dominant feature determining the electrocatalysis. Moreover, for the formic acid oxidation reaction, it has been shown that the behaviour of these steps reproduces the behaviour of the (110) sites on the polycrystalline electrodes. In fact, the measured currents for the polycrystalline samples can be considered as a linear combination of the Pt(n,n,n-2) and the Pt(100) surfaces, depending on the ratio of the dominant site on the surface [29]. Thus, the measured activity for both paths on polycrystalline samples with a large amount of (100) ordered domains will be very close to that of the Pt(100) electrode, whereas when the dominant domains on the sample have (111) symmetry, the behaviour will be closer to that of the Pt(n,n,n-2) electrodes with large terraces and, in the rest of cases, it will be close to the Pt(n,n,n-2) electrodes with short terraces.

Fig. 6 shows the summary of the voltammetric profiles for the Pt (10,10,9), Pt(997), and Pt(553) surfaces and the comparison with the Pt(111) electrode for a total concentration of formic acid of 0.5 M. The complete evolution with the concentration for each surface is presented in figures S3–S6. As has been already reported for sulfuric acid solutions, as the step density increases, the current decreases, and the onset of the oxidation shifts negatively for the positive scan direc-

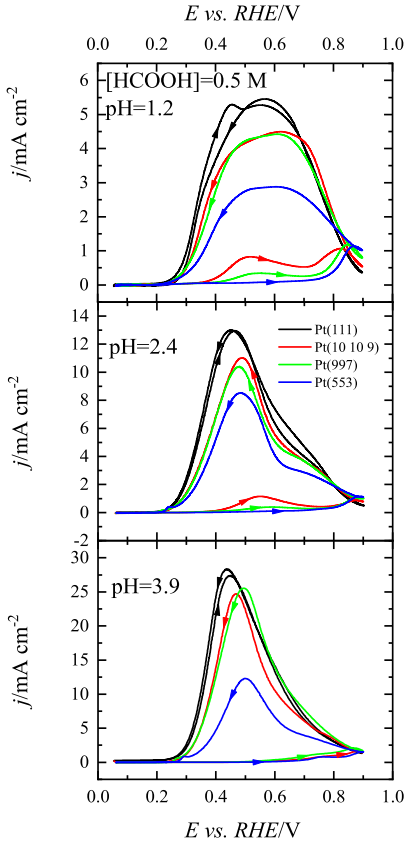

Fig. 6. Evolution of the voltammetric profile in HMRDE configuration of the stepped surfaces of the Pt(n,n,n-2) series with the step density in $HClO_4$/NaF buffered solutions of pH 1.2 (top), 2.4 (middle), and 3.9 (bottom). Arrows indicate the scan direction. The total formic acid concentration is 0.5 M. Scan rate: 50 mV s^{-1}; rotation rate: 1600 rpm.

tion. On the other hand, the shape of the voltammogram in the negative scan direction resembles that of the Pt(1 1 1) electrode. In the positive scan direction, currents are minimal, because CO_{ad} formation occurs on the step sites at $E < 0.2$ V, and the poisoning rate is proportional to the step density [19]. It can be observed that the currents in this scan direction follow the order Pt(10,10,9) > Pt(997) > Pt(553). When compared with the Pt(1 1 1) electrode, the behaviour in the negative scan direction with the concentration is essentially the same. In all cases, a change in the shape is observed from a broad wave that can be considered as the convolution of two different peaks with almost equal intensity to a situation in which the peak at lower potentials dominates. Also, the ratio between the currents of the stepped surfaces and the Pt(1 1 1) electrode is nearly independent of the pH, indicating that the reaction order for solution formate is 1 and that the overall mechanism is maintained.

4. Conclusions

A thorough analysis of the concentration dependence of the activity for the oxidation of formic acid at pH 1.2 and 3.9 on Pt(1 0 0), and on Pt(1 1 1) as well as on stepped Pt[*n*(1 1 1) × (1 1 0)] electrodes at pH 1.2, 2.4, and 3.9 has provided further evidence that formate, and not formic acid, is the active species, and that adsorbed monodentate formate is the active intermediate. On Pt(1 1 1), a reaction order 1 for formate (which, due to the acid-base equilibrium between HCOOH and $HCOO^-$, also results in a reaction order one for the total formic acid/-formate concentration when determined at constant potential and constant pH in the RHE scale) and a clear increase in the reaction rate with increasing pH were obtained, which is consistent with the mechanism proposed. On Pt(1 0 0), the competition between adsorbed hydrogen and formate for the adsorption sites cancels both the concentration and the pH dependence of the reaction rate. The potential dependence of the rate of dehydrogenation of formic acid to CO_{ad} on Pt(1 0 0) goes through a maximum both at pH 1.2 and pH 3.9, although the rate of dehydrogenation is slower and the maximum is broader at pH 3.9. The slower rate at the higher pH is consistent with the well-known fact that dehydrogenation of HCOOH is ad acid-catalysed reaction, but understanding the potential dependence of the dehydrogenation reaction at this pH will require further study. On Pt[*n*(1 1 1) × (1 1 0)] electrodes the behaviour observed is similar to that of Pt(1 1 1), only that now surface poisoning by CO_{ad} is faster due to the presence of (1 1 0) steps, and is again consistent with a reaction order 1 for formate.

CRediT authorship contribution statement

Mateusz J. Salamon: Investigation, Formal analysis, Writing - review & editing. **Valentín Briega-Martos:** Investigation, Methodology, Formal analysis, Writing - review & editing. **Angel Cuesta:** Conceptualization, Formal analysis, Funding acquisition, Writing - original draft, Writing - review & editing. **Enrique Herrero:** Conceptualization, Formal analysis, Funding acquisition, Writing - original draft, Writing - review & editing.

Data availability

Data will be made available on request.

Declaration of Competing Interest

The authors declare that they have no known competing financial interests or personal relationships that could have appeared to influence the work reported in this paper.

Acknowledgments

This research was funded by Ministerio de Ciencia e Innovación (Spain) (grant number PID2019-105653GB-I00), Generalitat Valenciana (Spain) grant number PROMETEO/2020/063. M.S. and A.C. gratefully acknowledge the support of the University of Aberdeen.

Appendix A. Supplementary data

Supplementary data to this article can be found online at https://doi.org/10.1016/j.jelechem.2022.116886.

References

[1] A. Capon, R. Parsons, The oxidation of formic acid at noble metal electrodes Part III. Intermediates and mechanism on platinum electrodes, J. Electroanal. Chem. 45 (1973) 205–231, https://doi.org/10.1016/S0022-0728(73)80158-5.
[2] E. Müller, S. Tanaka, Über die pulsierende elektrolytische Oxydation der Ameisensäure, Zeitschrift Für Elektrochemie Und Angewandte Physikalische, Chemie. 34 (1928) 256–264, https://doi.org/10.1002/bbpc.19280340510.
[3] E. Herrero, J.M. Feliu, Understanding formic acid oxidation mechanism on platinum single crystal electrodes, Curr Opin Electrochem. 9 (2018) 145–150, https://doi.org/10.1016/J.COELEC.2018.03.010.
[4] A. Cuesta, Formic acid oxidation on metal electrodes, in: K. Wandelt (Ed.), Encyclopedia of Interfacial Chemistry: Surface Science and Electrochemistry, Vol. 5, Elsevier, 2018, pp. 620–632.
[5] Y.-X. Chen, M. Heinen, Z. Jusys, R.J. Behm, Bridge-bonded formate: active intermediate or spectator species in formic acid oxidation on a pt film electrode?, Langmuir 22 (2006) 10399–10408
[6] A. Cuesta, G. Cabello, C. Gutierrez, M. Osawa, Adsorbed formate: the key intermediate in the oxidation of formic acid on platinum electrodes, PCCP 13 (2011) 20091–20095.
[7] A. Cuesta, G. Cabello, M. Osawa, C. Gutiérrez, Mechanism of the electrocatalytic oxidation of formic acid on metals, ACS Catal. 2 (2012) 728–738, https://doi.org/10.1021/cs200661z.

[8] A. Betts, V. Briega-Martos, A. Cuesta, E. Herrero, Adsorbed formate is the last common intermediate in the dual-path mechanism of the electrooxidation of formic acid, ACS Catal. 10 (2020) 8120–8130, https://doi.org/10.1021/acscatal.0c00791.

[9] J. Joo, T. Uchida, A. Cuesta, M.T.M. Koper, M. Osawa, Importance of acid-base equilibrium in electrocatalytic oxidation of formic acid on platinum, J Am Chem Soc. 135 (2013) 9991–9994, https://doi.org/10.1021/ja403578s.

[10] J. Joo, T. Uchida, A. Cuesta, M.T.M. Koper, M. Osawa, The effect of pH on the electrocatalytic oxidation of formic acid/formate on platinum: A mechanistic study by surface-enhanced infrared spectroscopy coupled with cyclic voltammetry, Electrochim Acta. 129 (2014) 127–136, https://doi.org/10.1016/j.electacta.2014.02.040.

[11] J.V. Perales-Rondón, S. Brimaud, J. Solla-Gullón, E. Herrero, R. Jürgen Behm, J.M. Feliu, Further insights into the formic acid oxidation mechanism on platinum: ph and anion adsorption effects, Electrochim Acta. 180 (2015) 479–485.

[12] A. Ferre-Vilaplana, J.V. Perales-Rondón, C. Buso-Rogero, J.M. Feliu, E. Herrero, Formic acid oxidation on platinum electrodes: a detailed mechanism supported by experiments and calculations on well-defined surfaces, J. Mater. Chem. A. 5 (41) (2017) 21773–21784.

[13] Y. Jiao, Y. Qiu, L. Zhang, W.-G. Liu, H. Mao, H. Chen, Y. Feng, K. Cai, D. Shen, B.o. Song, X.-Y. Chen, X. Li, X. Zhao, R.M. Young, C.L. Stern, M.R. Wasielewski, R.D. Astumian, W.A. Goddard, J.F. Stoddart, Electron-catalysed molecular recognition, Nature 603 (7900) (2022) 265–270.

[14] R. Francke, R.D. Little, Electrons and holes as catalysts in organic electrosynthesis, ChemElectroChem. 6 (2019) 4373–4382, https://doi.org/10.1002/CELC.201900432.

[15] A. Studer, D.P. Curran, The electron is a catalyst, Nature Chem 6 (9) (2014) 765–773.

[16] J. Clavilier, D. Armand, S.G. Sun, M. Petit, Electrochemical adsorption behaviour of platinum stepped surfaces in sulphuric acid solutions, J. Electroanal. Chem. 205 (1-2) (1986) 267–277.

[17] E. Herrero, J.M. Orts, A. Aldaz, J.M. Feliu, Scanning tunneling microscopy and electrochemical study of the surface structure of Pt(10,10,9) and Pt(11,10,10) electrodes prepared under different cooling conditions, Surf Sci. 440 (1999) 259–270, https://doi.org/10.1016/S0039-6028(99)00813-4.

[18] V. Briega-Martos, G.A.B. Mello, R.M. Arán-Ais, V. Climent, E. Herrero, J.M. Feliu, Understandings on the inhibition of oxygen reduction reaction by bromide adsorption on Pt(111) electrodes at different ph values, J Electrochem Soc. 165 (2018) J3045–J3051, https://doi.org/10.1149/2.0081815JES/XML.

[19] V. Grozovski, V. Climent, E. Herrero, J.M. Feliu, Intrinsic activity and poisoning rate for HCOOH oxidation on platinum stepped surfaces, PCCP 12 (2010) 8822, https://doi.org/10.1039/b925472b.

[20] V. Grozovski, V. Climent, E. Herrero, J.M. Feliu, Intrinsic activity and poisoning rate for HCOOH oxidation at Pt(100) and vicinal surfaces containing monoatomic (111) steps, ChemPhysChem 10 (2009) 1922–1926, https://doi.org/10.1002/cphc.200900261.

[21] M.D. Maciá, E. Herrero, J.M. Feliu, Formic acid self-poisoning on adatom-modified stepped electrodes, Electrochim Acta. 47 (2002) 3653–3661, https://doi.org/10.1016/S0013-4686(02)00335-3.

[22] J.V. Perales-Rondón, E. Herrero, J.M. Feliu, On the activation energy of the formic acid oxidation reaction on platinum electrodes, J. Electroanal. Chem. 742 (2015) 90–96.

[23] J.V. Perales-Rondón, E. Herrero, J.M. Feliu, Effects of the anion adsorption and pH on the formic acid oxidation reaction on Pt(111) electrodes, Electrochim Acta. 140 (2014) 511–517.

[24] C.A.A. Angelucci, H. Varela, E. Herrero, J.M.M. Feliu, Activation energies of the electrooxidation of formic acid on Pt(100), J. Phys. Chem. C 113 (2009) 18835–18841, https://doi.org/10.1021/jp907723k.

[25] F.W. Hartl, H. Varela, A. Cuesta, The oscillatory electro-oxidation of formic acid: Insights on the adsorbates involved from time-resolved ATR-SEIRAS and UV reflectance experiments, J. Electroanal. Chem. 840 (2019) 249–254, https://doi.org/10.1016/J.JELECHEM.2019.04.015.

[26] T. Fujii, R. Hayashi, Y. Oshima, Analysis of acid-catalyzed dehydration of formic acid in hot compressed water based on density functional theory, J Supercrit Fluids. 84 (2013) 190–194, https://doi.org/10.1016/J.SUPFLU.2013.10.005.

[27] A. Rodes, E. Pastor, T. Iwasita, An Ftir Study on the Adsorption of Acetate at the Basal Planes of Platinum Single-Crystal Electrodes, Journal of Electroanalytical Chemistry. 376 (1994) 109–118. https://doi.org/Doi 10.1016/0022-0728(94)03585-7.

[28] K. Domke, E. Herrero, A. Rodes, J.M. Feliu, Determination of the potentials of zero total charge of Pt(100) stepped surfaces in the [011] zone. Effect of the step density and anion adsorption, J. Electroanal. Chem. 552 (2003) 115–128, https://doi.org/10.1016/S0022-0728(02)01471-7.

[29] V. Grozovski, J. Solla-Gullón, V. Climent, E. Herrero, J.M. Feliu, Formic acid oxidation on shape-controlled Pt nanoparticles studied by pulsed voltammetry, J. Phys. Chem. C 114 (2010) 13802–13812, https://doi.org/10.1021/jp104755b.